Original Research

Guided bone regeneration produced by new mineralized and reticulated collagen membranes in critical-sized rat calvarial defects

Denusa M Veríssimo[1], Renata FC Leitão[2], Sônia D Figueiró[3], Júlio C Góes[3], Vilma Lima[1], Charles O Silveira[4] and Gerly AC Brito[2]

[1]Department of Physiology and Pharmacology, Federal University of Ceará, Fortaleza 60.430-270, Brazil; [2]Department of Morphology, School of Medicine, Federal University of Ceará, Fortaleza 60.430-270, Brazil; [3]Physics Department, Federal University of Ceará, Fortaleza 60.430-270, Brazil; [4]School of Medicine, Federal University of Ceará, Fortaleza 60.430-270, Brazil
Corresponding author: Denusa M Veríssimo. Email: denusa.verissimo@terra.com.br

Abstract

The aim of this study was to evaluate the bone regenerative effect of glutaraldehyde (GA) cross-linking on mineralized polyanionic collagen membranes in critical-sized defects on rat calvarias. Bone calvarial defects were induced in Wistar rats, which were then divided into five groups: a sham group; a control group, which received a commercial membrane; and GA, 25GA, and 75GA groups, which received one of three different polyanionic collagen membranes mineralized by 0, 25, or 75 hydroxyapatite cycles and then cross-linked by GA. Bone formation was evaluated based on digital radiography and computerized tomography. Histological analyses were performed 4 and 12 weeks after the surgical procedure to observe bone formation, membrane resorption, and fibrous tissue surrounding the membranes. Measurement of myeloperoxidase activity, tumor necrosis factor alpha, and interleukin 1beta production was performed 24 h after surgery. The percentage of new bone formation in the GA, 25GA, and 75GA groups was higher compared with the control and sham groups. In the GA and 25 GA groups, the membranes were still in place and were contained in a thick fibrous capsule after 12 weeks. No significant difference was found among the groups regarding myeloperoxidase activity and interleukin 1beta levels, although the GA, 25GA, and 75GA groups presented decreased levels of tumor necrosis factor alpha compared with the control group. These new GA cross-linked membranes accelerated bone healing of the calvarium defects and did not induce inflammation. In addition, unlike the control membrane, the experimental membranes were not absorbed during the analyzed period, so they may offer advantages in large bone defects where prolonged membrane barrier functions are desirable.

Keywords: Biomaterial(s), bone regeneration, collagen(s), guided bone regeneration, tissue engineering

Experimental Biology and Medicine **2015; 240: 175–184. DOI: 10.1177/1535370214549518**

Introduction

For predictable osseointegration of dental implants and good aesthetics, the presence of sufficient bone is necessary. Bone deficiency is, therefore, a major problem, and an extensive number of treatment modalities for alveolar ridge augmentation have been attempted as solutions. In guided bone regeneration, a barrier membrane prevents the in-growth of fibroblasts and provides a space for osteogenesis within the clot.[1,2] Although different barrier membranes have been developed, an ideal barrier membrane is not yet available.

Collagen membranes have excellent cell affinity and biocompatibility for tissue regeneration.[3] Membranes made from non-mineralized collagen, however, are normally of low strength and are thus difficult to manipulate. Furthermore, mineralized collagen is considered to provide better biocompatibility with animal and human bony tissue than pure collagen.[4] As a hard tissue implant material, mineralized collagen also displays a conductivity effect that enhances bone growth. The rate of resorption in collagen membranes can be controlled by changing the content of calcium phosphate minerals.[3] Mineralized collagen materials facilitate bone regeneration, inducing migration of undifferentiated cells into the graft recipient site, where they differentiate into osteoblasts and form new bone (i.e. stimulation of cellular transformation).[5] The composites also supply a ready source of calcium for rapid mineralization.[6,7] It has been reported that carboxyl group-containing organic polymers form apatite on their surfaces in

simulated body fluid if their carboxyl groups have been previously combined with calcium ions, because the carboxyl group induces apatite nucleation and releases calcium ions to accelerate this nucleation.[8,9]

The mechanical, chemical, and biological properties of collagen scaffolds can be influenced by modification of the matrix structure by chemical treatment with glutaraldehyde (GA), which is a reference agent for the cross-linking reactions. The *in vivo* resorption of collagen biomaterials can be controlled by this cross-linking reaction. Some authors have used arrays of collagen cross-linked with GA in the growth of fibroblasts with high biological efficiency.[10] GA reacts with the amino groups in the side chains of collagen molecules, creating a framework in the material that improves the mechanical and biological properties. Some problems related to GA cross-linking, such as polymerization of GA monomers in solution leading to heterogeneous cross-linking and cytotoxicity, have been overcome by continuous reaction with GA at low concentrations.[11] This method may produce a material with the same pattern of degradability, thus avoiding cytotoxic effects. In addition, progressive treatment with low concentrations of GA is believed to induce more homogeneous reactions in the collagen matrix.[12] Consistent with these reports, we recently demonstrated that the subcutaneous implantation in rats of mineralized polyanionic collagen (PAC) membranes cross-linked with GA led to a reduced inflammatory response and a lack of membrane resorption compared with implantation of membranes that were not cross-linked.[13]

The critical-size rat calvarium defect model has been used in several investigations to evaluate guided bone regeneration.[14–16] In rats, 5-mm calvarial defects are regarded as critical-size defects (CSDs). This model is useful for studying bone regeneration because it is relatively easy to manage and stage, and it has a low risk of complications. The model is relevant in periodontal research, as the embryonic origin of calvaria is similar to that of the mandible.[15] Without intervention, the defect will be filled with a fibrous connective tissue rather than with bone. The rat calvarial CSD model has been recommended for initial studies before subjecting higher phylogenetic species to testing.[17]

The goal of this research was to study the effect of three different PAC membranes, mineralized by alternate soaking processes in either 0, 25, or 75 hydroxyapatite cycles and cross-linked with GA, on the healing of rat calvarial bone defects. New bone formation, tissue inflammation, and resorption of these membranes were assessed.

Materials and methods

Collagen membrane

In the present study, PAC membranes from intestinal bovine serosa (PAC) were mineralized at 25°C for 0, 25, or 75 consecutive cycles with hydroxyapatite, at pH 9.0 and cross-linked with GA (GA, 25GA, and 75GA, respectively). The preparation of these PAC membranes as well as the methods for the mineralization and cross-linking with GA was described previously.[13] The membranes were manufactured by LOCEM, in the Physics Department of the Federal University of Ceará (Brazil). A collagen membrane of demineralized bovine cortical bone (Genderm, Genius, Baumer S.A., Brazil) was used as a control.

Animals

One hundred and ninety Wistar rats (Rattus norvegicus, albinus, Wistar) from the Federal University of Ceará, weighing 200–300 g, were housed in temperature-controlled rooms and received water and food *ad libitum*. All experimental protocols were in compliance with the Brazilian College for Animal Experimentation (COBEA) and the Institutional Animal Care and Use Committee guidelines of the Department of Physiology and Pharmacology, Federal University of Ceará, Brazil. The rats were housed in a room with a 12 h–12 h light–dark cycle at a temperature between 22°C and 24°C. The animals were randomly assigned to one of five experimental treatment groups:

(I) **Sham**: the surgical defects were not covered by a collagen membrane.
(II) **Control**: the surgical defects were covered by a commercial collagen membrane (Genderm, Baumer, Brazil).
(III) **GA**: the surgical defects were covered by a PAC membrane, without impregnation with hydroxyapatite and cross-linked with GA.
(IV) **25GA**: the surgical defects were covered by a PAC membrane, impregnated with 25 cycles of hydroxyapatite and cross-linked with GA.
(V) **75GA**: the surgical defects were covered by a PAC membrane, impregnated with 75 cycles of hydroxyapatite and cross-linked with GA.

Baseline. The animals sacrificed 24 h after the surgical procedure, from groups I, II, III, IV, and V provided baseline values of bone defects.

After general anesthesia, the overlying skin was shaved and disinfected with iodated alcohol. A semilunar incision was made in the scalp in the posterior region of the calvarium, allowing reflection of the skin, subcutaneous tissue, and periosteum in an anterior direction, exposing the parietal bones. A 5.25-mm diameter trephine bur was used in a slow-speed micromotor under constant saline irrigation to create a full thickness bone defect that included the sagittal suture. Attention was paid not to damage the underlying dura mater.

In all groups except the sham group, the surgical defect was covered with a disc (8-mm in diameter) of one of the control or PAC membranes. The soft tissues were then repositioned and sutured to achieve primary closure (4.0, Catgut). Each group of animals was euthanized after 24 h ($n = 6$ per group), four weeks ($n = 6$ per group), eight weeks ($n = 8$ per group), or 12 weeks ($n = 12$ per group) after the surgical procedure (a total of 160 animals) (Table 1). The areas of the original surgical defect and the surrounding tissues were removed *en bloc* and were fixed in 10% neutral

Table 1 Parameters of the analysis, time of sacrifice and number of animals used

Analysis	Time of sacrifice				Number of animals
	24 h (6 animals p/group)	4 weeks (6 animals p/group)	8 weeks (8 animals p/group)	12 weeks (12 animals p/group)	
New bone formation	X	X	X	X	160
Histological analysis	X	X	X	X	
MPO activity and cytokine dosage	X				30
Total of animals					190

formalin for 24 h. Then, digital radiography and computed tomography (CT) were used to analyze the blocks. Following these procedures, the specimens were rinsed with tap water and decalcified in 10% ethylediaminetetraacetic acid solution. Before the embedding procedure, each sample was split transversely through the middle of the bone defect to ensure that the microtome sections contained the area of interest. The specimens were then serially sectioned 4 μm to the original transverse section and stained with hematoxylin and eosin (H&E) for analysis by light microscopy. Within the most central portion of each defect, the section displaying the widest extension was identified for histological analysis.

Evaluation of new bone formation

Digital radiography imaging. Digital radiographs of all specimens were taken using a digital dental X-ray apparatus (Spectro 70X Seletronic, Dabi Atlante, São Paulo, SP, Brazil) and a digital sensor, using the following parameters: 8 mA, 70 kVp, focus and object distance of 8 cm, and exposure time of 0.1 s. The digital radiographic images of the specimens were then analyzed using NIHImageJ software. The radiolucent square area (pixel/mm) for each animal was measured, and a group mean area was calculated (pixel/mm).

The radiolucent mean area of each group was then computed as a percentage of the radiolucent mean area obtained from the animals sacrificed 24 h after surgery, considered as a reference for the original bone defect (referred as baseline group), according to a previously described formula[18]: mean of the radiolucent area of each group (4, 8, or 12 weeks) multiplied by 100, divided by the baseline radiolucent mean area. To calculate the percentage of the area of new bone formation, the obtained result was subtracted from 100 because the baseline radiolucent area is equivalent to 100%. The radiolucent area is inversely correlated with the new bone formed and is expressed as a fraction of the original area.

CT imaging. CT was taken using a PreXion 3D CT Scanner (PreXion Co., Ltd. Tokyo, Japan) (90 kV/4 mA, 608 × 616, 200-μm resolution), and the best visual resolution slice obtained from each specimen was selected for calculation of the radiolucent area (mm^2) using NIHImageJ software. The radiolucent mean area of each group was then determined 4 and 12 weeks after surgery to compare the amount of mineralized tissue produced in response to implantation of each tested membrane type. The radiolucent area is inversely related to bone formation, as bones have relative radiopacity in radiographs.

In addition, 12 weeks after surgery, the mineralized bone regeneration behavior was estimated by the radiographic density analysis of a 35-mm^2 area region of interest corresponding to the bone defect. The mean value of the radiographic density obtained for each group was expressed as grey levels. Radiographic density is the measure of the overall darkening of the image. Density is a logarithmic unit that describes the ratio between light hitting the film and light being transmitted through the film. A higher radiographic density results in more opaque areas on the film, and a lower density results in more transparent areas on the film. Thus, it can be concluded that the bone formation areas within defects correlate with increased radiographic density.

Histological analysis

Two histological sections from each animal, representing approximately the center of the original surgical defect, were selected for a blind histological evaluation of the resorption suffered by the membranes and of the presence of a fibrosis capsule involving these membranes. For this analysis, the images of the histological sections were captured by a digital camera connected to a light microscope with an original magnification of 40×. The animals in which membrane displacement was observed were excluded from histological, digital radiography, and CT analysis.

Myeloperoxidase activity in tissue surrounding the membranes

Myeloperoxidase (MPO) activity, a marker for the presence of neutrophils in inflamed tissue, was measured using a modified version of the method described by Bradley *et al*.[19] A sample of the soft tissue surrounding the surgical area (approximately 8-mm in diameter) was removed with a scalpel blade 24 h after the surgical procedure for analysis of MPO activity (a total of 30 animals). The specimens were stored at −70°C prior to being assayed. The tissues were weighed and triturated in an ice-cold buffer solution (hexadecyltrimethylammonium bromide-HTAB, Sigma) using a Polytron Ultraturrax, and the homogenate was centrifuged (4200 rpm) at 4°C for 15 min. The supernatant was collected for analysis by enzyme-linked immunosorbant assay

(ELISA), and values were expressed as units of MPO per mg of tissue.[19]

Cytokine (TNF-α, IL-1β) concentration in the tissue surrounding the membranes

A sample of the surrounding tissue was removed from the five groups after 24 h (from the same 30 animals used to determine the MPO activity) to evaluate the cytokine concentration. The specimens were stored at −70°C prior to being assayed. The collected tissue was homogenized and processed as described by SaWeh-Garabedian *et al*.[20] Tumor necrosis factor alpha (TNF-α) and interleukin 1beta (IL-1β) concentrations were determined by ELISA, as described previously.[21] Briefly, microtiter plates were coated overnight at 4°C with antibodies against rat TNF-α and IL-1β (2 μg/mL) (Kit DuoSet – R&D Systems). After blocking the plates, the samples and standard were added at various dilutions in duplicate and incubated at 4°C for 24 h. The plates were washed three times with buffer, and then biotinylated sheep polyclonal anti-TNF-α and anti-IL-1β (Kit DuoSet – R&D Systems) (diluted 1:1000 with assay buffer containing 1% bovine serum albumin) were added to the wells. After further incubation at room temperature for 1 h, the plates were washed, and 50 μl of avidin–horseradish peroxidase (diluted 1:5000) was added to the plates. An aliquot of 50 μL of the color reagent o-phenylenediamine was added 15 min later, and the plates were incubated in the dark at 37°C for 15–20 min. The enzyme reaction was terminated by addition of H_2SO_4 (sulfuric acid), and the absorbance was measured at 490 nm. The measured values were expressed as picograms per milliliter (pg/mL).

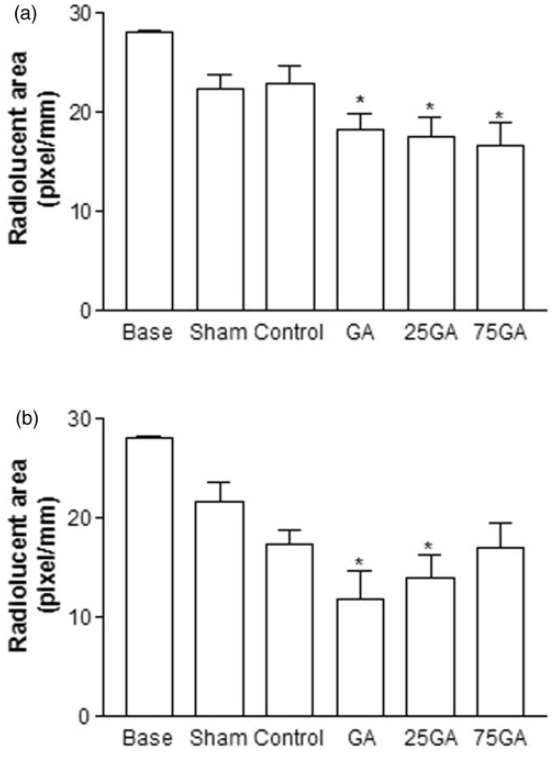

Figure 1 Radiolucent area measured by digital radiography 4 (a) and 12 (b) weeks after the surgical procedure. The mean value of the radiographic radiolucent area was measured and calculated by comparing the amount of mineralized tissue produced in each membrane group. Bars represent the mean value ± standard error of the mean (SEM). *$P < 0.05$ represents significant difference compared with the baseline group (24 h after the surgical procedure). Data were analyzed by ANOVA and the Bonferroni test

Statistical analysis

Univariate analysis of variance (ANOVA) followed by Bonferroni's test was used to compare the mean observed values. $P < 0.05$ was considered to indicate a significant difference. Both analyses were performed using Prism 3 software (Graph-Pad Software, USA).

Results

Evaluation of new bone formation

Digital radiography imaging. Four weeks after the surgical procedure, the GA, 25GA, and 75GA groups exhibited a smaller radiolucent area that was statistically different compared with the baseline group (radiolucent area 24 h after the surgical procedure) (*$P < 0.05$). On the contrary, the sham and the control groups showed no statistical difference compared to baseline group (Figure 1(a)). Similarly, 12 weeks after the surgical procedure, the experimental groups GA and 25GA, unlike the sham, control, and 75GA groups, exhibited a significant decrease in radiolucent areas compared with the baseline group (Figure 1(b)). There was no statistical difference between the GA, 25GA, and 75GA groups and the control group after 4 and 12 weeks of observation.

Figure 2 shows the percentage of new bone formation 4, 8, and 12 weeks after the surgical procedure. At four weeks, the percentage of new bone formation noted in all experimental groups (GA, 25GA and 75GA) was approximately 40%, which was higher than that found in both the control and sham groups (approximately 20%). Analysis of bone formation performed 8 and 12 weeks after the surgery yielded similar results. An increase in bone formation (40% to 50%) was observed in all experimental groups; in the sham group, bone formation remained approximately 20%. The GA group showed the highest percentage (approximately 50%) of new bone formation during the 12-week observation period (Figure 2).

Reinforcing the results from digital radiography, four weeks after the surgical procedures, only the GA, 25GA, and 75GA groups exhibited a significantly smaller radiolucent area compared with the baseline group (* $P < 0.05$) (Figure 3(a)). Twelve weeks after the procedure, only the GA and 25GA groups, but not the other experimental groups, exhibited significant differences compared with the baseline group (*$P < 0.05$) (Figure 3(b)).

Figure 4 shows the radiographic density 12 weeks after implantation of the membranes. The GA, 25GA, 75GA, and control groups had similar densities and exhibited significant differences compared with the sham group (**$P < 0.05$).

Figure 5 shows the images displayed by digital radiography and CT 12 weeks after the surgical procedures. The images obtained by CT clearly had a higher definition of the surgical wound than did the images obtained by digital radiography.

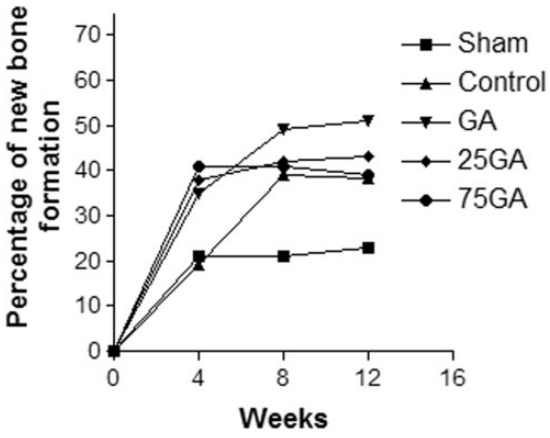

Figure 2 Percentage of new bone formation after the surgical procedure during the evaluated period. The radiolucent area for each group was calculated as a percentage of the respective baseline area (24 h) measurement according to the following formula: mean of the radiolucent area of each group 4, 8 and 12 weeks after the surgical procedure multiplied by 100, divided by the radiolucent mean area of the baseline group. Subsequently, the percentage of new bone formation area was calculated and compared. The radiolucent area of the baseline group is equivalent to 100%, and the result was reduced by 100 to correspond to the new bone formation data

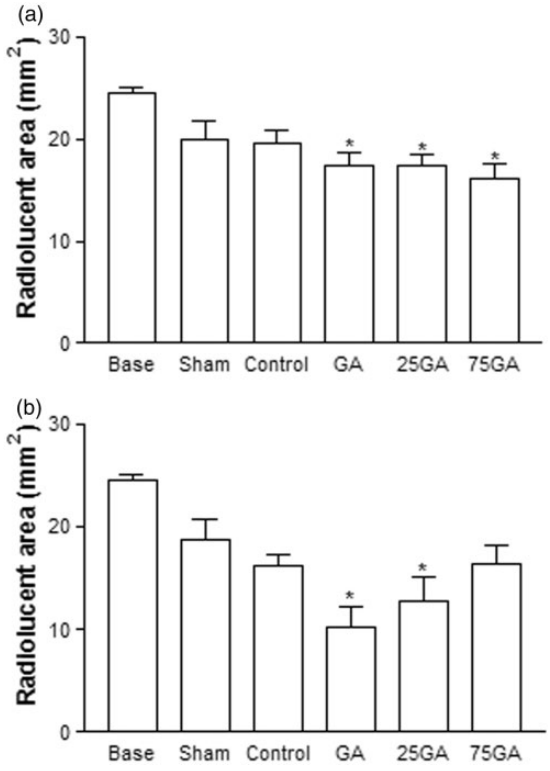

Figure 3 Radiolucent area measured by computed tomography 4 (a) and 12 (b) weeks after the surgical procedure. The mean value of the radiographic radiolucent area was measured and calculated by comparing the amount of mineralized tissue produced in each group. Bars represent the mean value ± standard error of the mean (SEM). $^{*}P < 0.05$ represents significant difference compared with the baseline group (24 h after the surgical procedure). Data were analyzed by ANOVA and the Bonferroni test

Histological analysis

The histological analysis of the area corresponding to the surgical defect performed four weeks after the procedure revealed a marked resorption of the membranes in the control group. In the experimental groups GA and 25GA, the membranes remained intact, while the membranes in the 75GA group showed signs of resorption. Twelve weeks after surgery, the membranes in the control group had been completely absorbed (Figure 6(b)), and the membranes in the 75GA group were in the advanced state of resorption (Figure 6(e)). However, the membranes in the GA and 25GA groups were preserved (Figure 6(c) and (d), respectively). The histological evaluation also revealed a fibrous capsule surrounding the membranes of the GA and 25GA groups, observed four weeks and 12 weeks (Figure 6(c) and (d), respectively) after the surgical procedures. There were no fibrous capsules in the control group at any of the observation periods (Figure 6(b)). In the 75GA group, the fibrous capsule tended to disappear as the membranes are resorbed (Figure 6(e)). Histological evaluation showed new bone formation in all groups 12 weeks after surgical procedure (Figure 6).

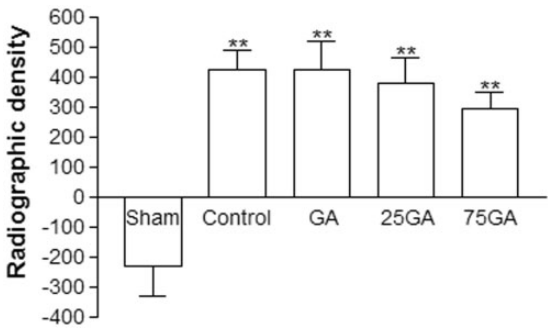

Figure 4 Radiographic density 12 weeks after the surgical procedure. The mean value of the radiographic density was measured and calculated by comparing the amount of mineralized tissue produced in response to each membrane used. Bars represent the mean value ± standard error of the mean (SEM). $^{**}P < 0.05$ represents significant difference compared with the sham group. Data were analyzed by ANOVA and the Bonferroni test

MPO activity and cytokine (TNF-α, IL-1ß) concentration in the tissue surrounding the membranes

No significant differences among the groups were found regarding MPO activity and pro-inflammatory cytokine IL-1β content 24 h after the surgery (Figure 7(a) and (b)). However, a marked decrease in TNF levels was observed 24 h after surgery in the GA, 25GA, and 75GA groups relative to the control group ($P < 0.05$) (Figure 7(c)).

Discussion

The present study clearly demonstrates the bone-healing efficacy of three different collagen membranes. These membranes were mineralized by alternative soaking processes for 0, 25, or 75 hydroxyapatite cycles and cross-linked by GA. Studies were performed using the critical-size rat calvarium defect model. This experimental model for studying bone regeneration is stable and relatively easy to manage, and it has a low risk of complications.[15] The size of the bone calvarium defects (5 mm diameter) was in agreement with previous studies of CSDs in rats.[22–25] Bone formation was

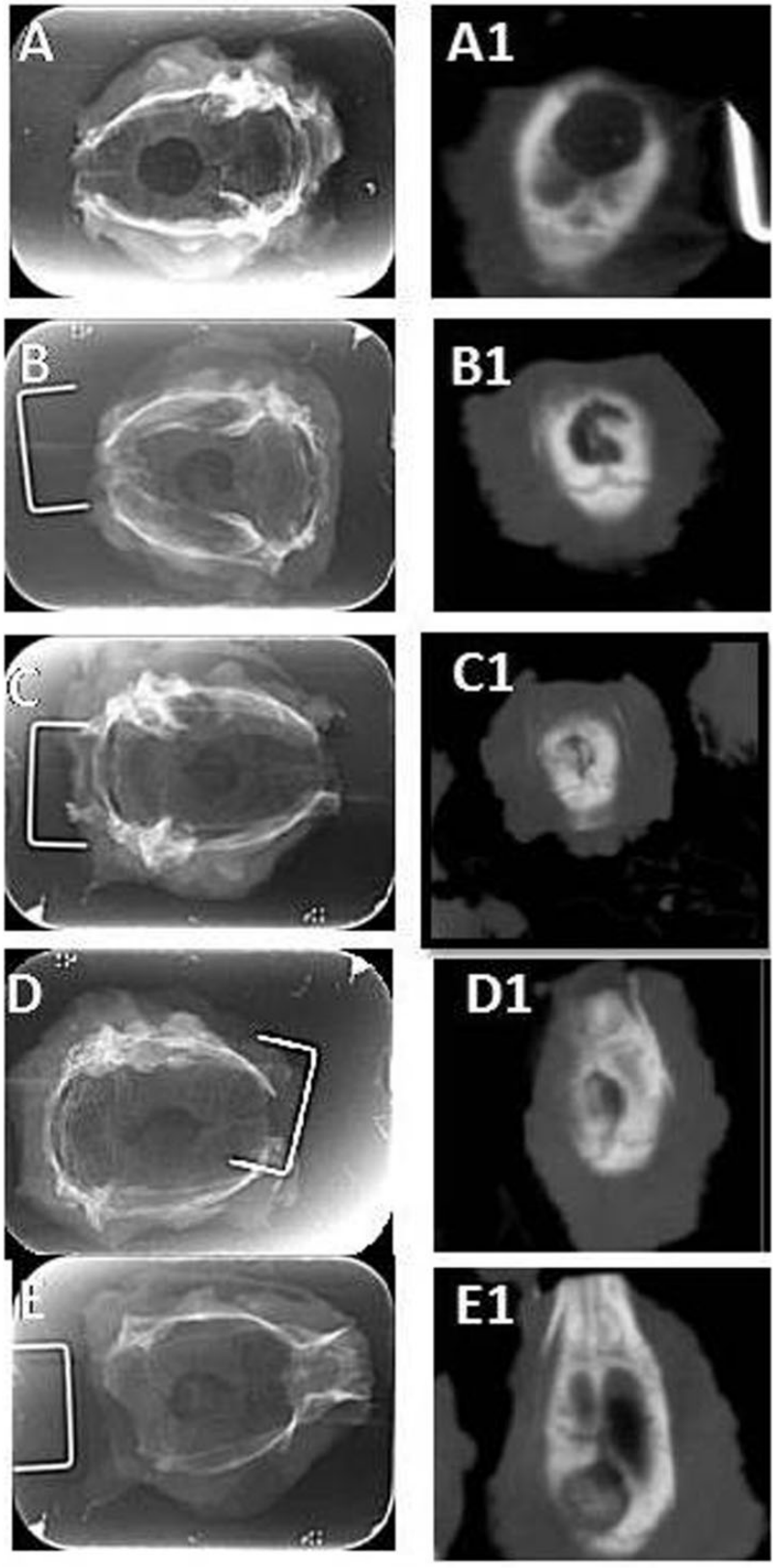

Figure 5 Comparison between the images obtained by digital radiography and computed tomography 12 weeks after the surgical procedure. The images correspond to: (a) the sham group, (b) the control group, (c) the GA group, (d) the 25GA group and (e) the 75 GA group. Images a, b, c, d and e correspond to digital radiography; the images a1, b1, c1, d1 and e1 correspond to computed tomography scans

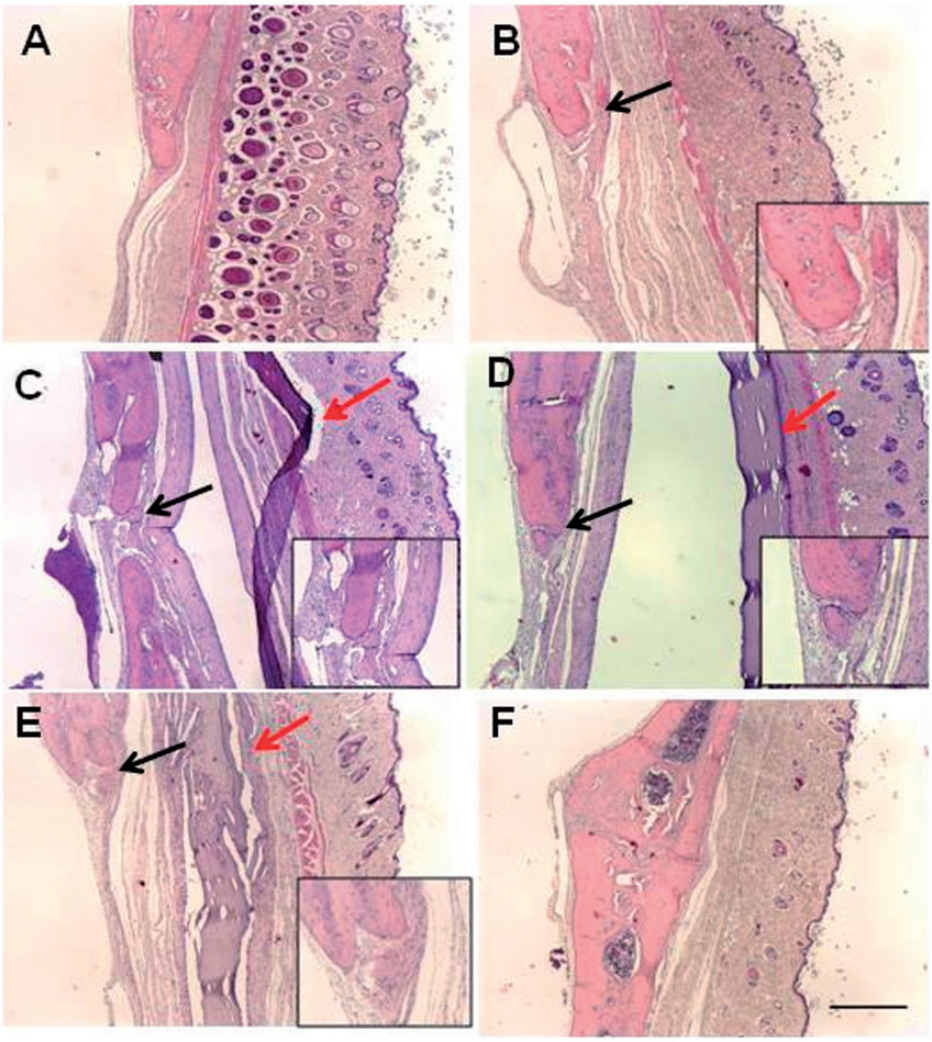

Figure 6 Microscopic aspects of the rat tissues after induction of 5-mm critical-sized cranial defects. Twelve weeks after the surgical procedure, the calvaria, the membrane and the surrounding tissue were removed and processed for hematoxylin and eosin staining. The photomicrographs represent (a) the sham group, (b) the control group, (c) the GA group, (d) the 25GA group, (e) the 75GA group and (f) non-operated animals. Black arrows represent newly formed bone. Red arrows represent membranes of different groups. Scale bar length, 250 μm (×40 magnification). Magnifications represent areas of new bone formation. (A color version of this figure is available in the online journal.)

assessed by tomography, a more desirable method to evaluate bone formation during the wound healing process than digital radiography and microscopy of histological slides.[26,27]

The GA and 25GA groups showed the best results 12 weeks after the surgery, exhibiting significant differences compared with the baseline group, which represents the original bone defect. However, a complete closure of the calvarial defect was not observed in this study. Twelve weeks after surgery, the amount of new bone formation in the GA, 25GA, and 75GA groups was around 40% to 50% of the original defect and they had similar densities, suggesting that the tested membranes have effects on bone quality that were similar to those of the control membrane.The shallow geometry of a calvarial defect requires a barrier membrane with superior mechanical properties to prevent collapse and subsequent impairment of bone regeneration in the defect.[28] Although the literature reports that nanocarbonated hydroxyapatite/collagen composite materials facilitate reliable bone regeneration, our data do not show statistical differences at any observation time in bone formation among the groups that received membranes impregnated with hydroxyapatite (25GA and 75GA groups) and the GA group, which consisted of animals that received non-mineralized membranes. Hydroxyapatite did not substantially enhance the healing of calvarial defects in the current study. We speculate that the process of crosslinking with GA must have promoted a closing of the membrane fiber, thus preventing the release of hydroxyapatite crystals into the site. In addition, the data showed that regular apatite coating had formed larger tangles of bundles within the collagen fibrils that were a few hundred nanometers in size;[9] thus, it is unlikely that the materials in this work contained the nano-apatites necessary for supporting osteoblast-like cell proliferation and differentiation.[29]

In the present study, the commercial collagen membrane of demineralized bovine cortical bone, which was used as a

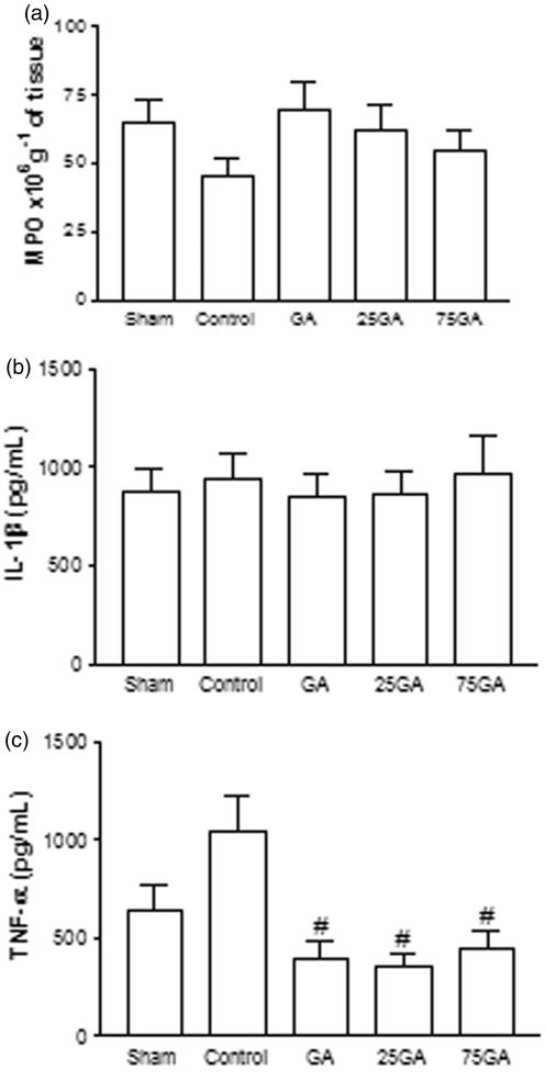

Figure 7 Myeloperoxidase activity and cytokine concentration in the tissue surrounding the critical-sized defect in rats. After animals were sacrificed, a sample of the tissue surrounding the defect was harvested for the MPO activity assay (a) and for the analysis of the levels of the cytokines TNF-α (b) and IL-1β (c) 24 h after the surgical procedure. Bars represent the mean value ± standard error of the mean (SEM). #$P < 0.05$ represents significant difference compared with the control group. Data were analyzed with ANOVA and the Bonferroni test

control, was still present four weeks after the implantation, despite it showing intense signs of resorption. Twelve weeks later, that membrane was completely resorbed. This finding was expected because the resorption of commercially available collagen membranes has been reported to occur within the first two months after treatment.[30] In the subcutaneous tissue of rats, the resorption of this commercial collagen membrane begins very early and is completely absorbed by day 15.[13] The difference in the resorption time of the commercial membrane reported in these two studies may be due to the reduced vascular tissue found in the skull compared with the subcutaneous tissue of the dorsal region.[14]

The literature has suggested that differences in the resorption pattern may have clinical implications. In guided bone regeneration, a common procedure in dental implant surgery, barrier membranes are used to exclude epithelial and connective tissue and to allow the proliferation of the bone progenitor cells into the isolated area.[18,31–33] In this case, bioabsorbable and non-absorbable membranes are effective.[31,34,35] However, non-absorbable membranes, mostly composed of polytetrafluoethylene, require a second surgical procedure for their removal.[18,36–39] Therefore, bioabsorbable membranes with comparable clinical outcomes have become popular in bone-regeneration procedures.[35,36] Successful regeneration is possible if soft tissue is excluded and space for bone growth is maintained throughout the healing time. This can vary between 3 and 12 months, depending on the dimensions of the bone defect.[31,32,40] Premature membrane resorption leads to less-than-optimal results.[18] The membranes should be chosen according to the clinical demands of each case. Thus, in large, non-self-contained bone defects, where prolonged membrane barrier functions are desirable, certain cross-linked membranes may offer advantages. In this context, the experimental GA cross-linked membranes are an attractive option when the production of new bone depends on the prolonged survival of a mechanical barrier. The preservation of the membrane, secondary to formation of the fibrous capsule, may be important for bone regeneration, as the GA and 25GA groups displayed better bone formation than did the 75GA group. Moreover, the premature resorption observed in the 75GA group may be explained by the possibility of having a lower amount of GA available for collagen crosslinking due to the physical barrier created by the hydroxyapatite, suggesting the necessity of reducing the number of hydroxyapatite impregnation cycles. A membrane with 50 cycles of hydroxyapatite impregnation could achieve better results and might be tested. As another option, the crosslinking could be done before the mineralization, so GA binds lysine, which contains positive charges, and then negative charges makes available the aspartic and glutamic acids, to serve as binding sites for calcium. Consumption of positive charges by crosslinking may even improve the efficiency of mineralization.[9]

The application of the tested experimental membranes is reinforced by the current results showing that those membranes do not trigger a significant inflammatory reaction. Such inflammation was evaluated by MPO activity, a marker for neutrophils in inflamed tissue, and by the concentration of the pro-inflammatory cytokines IL-1β and TNF-α in the circumjacent subcutaneous calvarium tissue. A marked decrease in TNF levels among the experimental groups compared with the control group suggests a better biocompatibility of the tested membranes. Moreover, the histological evaluation of the all groups showed discrete accute inflammatory cell infiltration (neutrophils) at 24 h. Four, eight, and 12 weeks after the surgery, few mononuclear cells and osteoclasts were observed at the edges of the wound, in all groups. Mild inflammation may stimulate osteoclastic resorption, as osteoclasts respond to inflammatory mediators such as IL-1β and TNF-α.[41] Consistent with these data, we have previously demonstrated that GA cross-linked membranes reduce the inflammatory response in the rat subcutaneous implant model.[13]

Conclusion

According to our results, the GA cross-linked membranes were as effective as the tested commercial collagen membrane at regenerating bone in injured rat calvarias. In view of this, the GA cross-linked membranes may offer advantages in large bone defects where prolonged membrane barrier functions are desirable. The impregnation of the collagen membranes with hydroxyapatite did not positively affect the amount of new bone regeneration in the current study.

Authors contributions: All seven authors have read and approved the manuscript and have contributed significantly to this work.

ACKNOWLEDGEMENTS

The authors thank Conceição da Silva Martins and Maria do Socorro França Monte, Department of Morphology, Faculty of Medicine, Federal University of Ceará, Brazil, for providing technical assistance and Perboyre Castelo in Dentistry Radiology for radiological assistance. This work was supported by Grant INCT 573928/2008-8 and Fundação Cearense de Apoio ao Desenvolvimento Científico e Tecnológico (FUNCAP).

REFERENCES

1. Hollinger JO, Buck DC, Bruder SP. Biology of bone healing: its impact on clinical therapy. In: Lynch SE, Genco RJ, Marx RE (eds). *Tissue engineering. Applications in maxillofacial surgery and periodontics*, 1st ed. Chicago: Quintessence, 1999, pp. 17–53
2. Bunyaratavej P, Wang HL. Collagen membranes: a review. *J Periodontol* 2001;**72**:215–29
3. Liao S, Wang W, Uo M, Ohkawa S, Akasaka T, Tamura K, Cui F, Watari F. A three-layered nano-carbonated hydroxyapatite/collagen/PLGA composite membrane for guided tissue regeneration. *Biomaterials* 2005;**26**:7564–71
4. Zhu X, Eibl O, Scheideler L, Geis-Gerstorfer J. Characterization of nano hydroxiapatite/collagen surfaces and cellular behaviors. *J Biomed Mater Res A* 2006;**79**:114–27
5. Kikuchi M, Itoh S, Ichinose S, Shinomiya K, Tanaka J. Self organization mechanism in a bone-like hydroxyapatite/collagen nanocomposite synthesized in vitro and its biological reaction in vivo. *Biomaterials* 2001;**22**:1705–11
6. Du C, Cui FZ, Zhang W, Feng QL, Zhu XD, de Groot K. Formation of calcium phosphate/collagen composites through mineralization of collagen matrix. *J Biomed Mater Res* 2000;**50**:518–27
7. Chang MC, Ikoma T, Kikuchi M, Tanaka J. Preparation of a porous hydroxyapatite/collagen nanocomposite using glutaraldehyde as a crosslinkage agent. *J Mater Sci Lett* 2001;**20**:1199–201
8. Kawashita M, Nakao M, Minoda M, Kim HM, Beppu T, Miyamoto T, Kokubo T, Nakamura T. Apatite-forming ability of carboxyl group-containing polymer gels in a simulated body fluid. *Biomaterials* 2003;**24**:2477–84
9. Góes JC, Figueiró SD, Oliveira AM, Macedo AA, Silva CC, Ricardo NM, Sombra AS. Apatite coating on anionic and native collagen films by an alternate soaking process. *Acta Biomater* 2007;**3**:773–8
10. Chen G, Sato T, Ohgushi H, Ushida T, Tateishi T, Tanaka J. Culturing of skin fibroblasts in a thin PLGA–collagen hybrid mesh. *Biomaterials* 2005;**26**:2559–66
11. Yoshioka SA, Goissis G. Thermal and spectrophotometric studies of new crosslinkingmethod for collagen matrix with glutaraldehyde acetals. *J Mater Sci: Mater Med* 2008;**19**:1215–23
12. Goissis G, Braile DM, Carnevalli NC, Ramireza VA. Thermal and morphological properties of glutaraldehyde crosslinked bovine pericardium followed by glutamic acid treatment. *Mater Res* 2009;**12**:113–9
13. Veríssimo DM, Leitão RFC, Ribeiro RA, Figueiró SD, Sombra ASB, Góes JC, Brito GAC. Polyanionic collagen membranes for guided tissue regeneration: effect of progressive glutaraldehyde cross-linking on biocompatibility and absorption. *Acta Biomaterialia* 2010;**6**:4011–8
14. Schmitz JP, Hollinger JO. The critical size defect as an experimental model for craniomandibular nonunions. *Clin Orthop* 1986;**205**:299–308
15. Bosch C, Melsen B, Vargervik K. Importance of the critical-size bone defect in testing bone-regenerating materials. *J Craniofac Surg* 1998;**9**:310–6
16. Verna C, Bosch C, Dalstra M, Wikesjo UME, Trombelli L. Healing patterns in calvarial bone defects following guided bone regeneration in rats: a microCT analysis. *J Clin Periodontol* 2002;**29**:865–87
17. Hollinger JO, Kleinschmidt JC. The critical size defect as an experimental model to test bone repair materials. *J Craniofac Surg* 1990;**1**:60–8
18. Moses O, Vitrial D, Aboodi G, Sculean A, Tal H, Kozlovsky A, Artzi Z, Weinreb M, Nemcovsky CE. Bioabsorption of three different collagen membranes in the rat calvarium: a comparative study. *J Periodontol* 2008;**79**:905–11
19. Bradley PP, Christensen RD, Rothstein G. Cellular and extracellular myeloperoxidase in pyogenic inflammation. *Blood* 1982;**60**:618–22
20. SaWeh-Garabedian B, Poole S, Allchorne A, Winter J, Woolf CJ. Contribution of interleukin-1 beta to the inflammation-induced increase in nerve growth factor levels and inflammatory hyperalgesia. *Br J Pharmacol* 1995;**115**:1265–75
21. Cunha FQ, Boukili MA, Motta JIB, Vargaftig BB, Ferreira SH. Blockade by fenspiride of endotoxin-induced neutrophil migration in the rat. *Eur J Pharmacol* 1993;**238**:47–52
22. Mardas N, Kostopoulos L, Karring T. Bone and suture regeneration in calvarial defects by e-PTFE-membranes and demineralized bone matrix and the impact on calvarial growth: an experimental study in the rat. *J Craniofac Surg* 2002;**13**:453–64
23. Furlaneto FA, Nagata MJ, Fucini SE, Deliberador TM, Okamoto T, Messora MR. Bone healing in critical size defects treated with bioactive glass/calcium sulfate: a histologic and histometric study in rat calvaria. *Clin Oral Implants Res* 2007;**18**:311–8
24. Kozlovsky A, Aboodi G, Moses O, Tal H, Artzi Z, Weinreb M, Nemcovsky CE. Bio-degradation of a resorbable collagen membrane (Bio-Gides) applied in a double-layer technique in rats. *Clin Oral Impl Res* 2009;**20**:1116–23
25. Potijanyakul P, Sattayasansakul W, Pongpanich S, Leepong N, Kintarak S. Effects of enamel matrix derivative on bioactive glass in rat calvarium defects. *J Oral Implantol* 2010;**36**:195–205
26. Yeom HR, Blanchard S, Kim SJ, Zunt S, Chu TMG. Correlation between micro-computed tomography and histomorphometry for assessment of new bone formation in a calvarial experimental model. *J Craniofac Surg* 2008;**19**:446–52
27. Pryor ME, Susin C, Wikesjö UM. Validity of radiographic evaluations of bone formation in a rat calvaria osteotomy defect model. *J Clin Periodontol* 2006;**33**:455–60
28. Dupoirieux L, Pourquier D, Picot MC, Neves M. Comparative study of three different membranes for guided bone regeneration of rat cranial defects. *Int J Oral Maxillofac Surg* 2001;**30**:58–61
29. Yang F, Both SK, Yang X, Walboomers XF, Jansen JA. Development of an electrospun nano-apatite/PCL composite membrane for GTR/GBR application. *Acta Biomater* 2009;**5**:3295–304
30. Schliephake H, Tavassol F, Gehnsky M, Dard M, Sewing A. Use of a mineralized collagen membrane to enhance repair of calvarial defects in rats. *Clin Oral Impl Res* 2004;**15**:112–8
31. Nyman S, Gottlow J, Lindhe J, Karring T, Wennström J. New attachment formation by guided tissue regeneration. *J Periodontal Res* 1987;**22**:252–4
32. Schlegel AK, Mohler H, Busch F, Mehl A. Preclinical and clinical studies of a collagen membrane (BioGide). *Biomaterials* 1997;**18**:535–8
33. Greenstein G, Caton JG. Biodegradable barriers and guided tissue regeneration. *Periodontol 2000* 1993;**1**:36–45

34. Patino MG, Neiders ME, Andreana S, Noble B, Cohen RE. Collagen as an implantable material in medicine and dentistry. *J Oral Implantol* 2002;**28**:220–5
35. Moses O, Pitaru S, Artzi Z, Nemcovsky CE. Healing of dehiscence-type defect in implant placed together with different barrier membranes: a comparative clinical study. *Clin Oral Implants Res* 2005;**16**:210–9
36. Simion M, Trisi P, Maglione M, Piattelli A. A preliminary report on a method for studying the permeability of expanded polytetrafluoroethylene membrane to bacteria in vitro: a scanning electron microscopic and histological study. *J Periodontol* 1994;**65**:755–61
37. Simion M, Masitano U, Salvato A. Treatment of dehiscences and fenestration around dental implants using resorbable and non-resorbable membranes associated with bone autografts: a comparative clinical study. *Int J Oral Maxillofac Implants* 1997;**12**:159–67
38. Nowzari H, Slots J. Microscopic and clinical study of polytetrafluoroethylene membranes for guided bone regeneration around implants. *Int J Oral Maxillofac Implants* 1995;**10**:67–73
39. Nowzari J, Engebretson SP, Donath K, Weber HP. Guided bone regeneration utilizing expanded polytetrafluoroethylene membranes in combination with submerged and non submerged dental implants in beagle dogs. *J Periodontol* 1998;**69**:528–35
40. Hammerle CH, Chiantella GC, Karring T, Lang NP. The effect of deproteinized bovine bone mineral on bone regeneration around titanium dental implants. *Clin Oral Implants Res* 1998;**9**:151–62
41. Kobayashi K, Takahashi N, Jimi E, Udagawa N, Takami M, Kotake S, Nakagawa N, Kinosaki M, Yamaguchi K, Shima N, Yasuda H, Morinaga T, Higashino K, Martin JT, Suda T. Tumor necrosis factor a stimulates osteoclast differentiation by a mechanism independent of the ODF/RANKL-RANK interaction. *J Exp Med* 2000;**191**:275–85

(Received October 6, 2013, Accepted August 4, 2014)